Mammalian sprouty proteins assemble into large monodisperse particles having the properties of intracellular nanobatteries

Xinle Wu*, Peter B. Alexander*, Ying He*, Masahide Kikkawa†, Pia D. Vogel‡, and Steven L. McKnight*§

Departments of *Biochemistry and †Cell Biology, University of Texas Southwestern Medical Center, 5323 Harry Hines Boulevard, Dallas, TX 75390; and ‡Department of Biological Sciences, Southern Methodist University, 6501 Airline Road, Dallas, TX 75275

Contributed by Steven L. McKnight, August 5, 2005

Sprouty proteins act as intracellular inhibitors of receptor tyrosine kinase signaling. Here we show that the mammalian Sprouty2 protein contains an iron–sulfur complex that can exist in an oxidized, reduced, or nitrosylated state. Purified Sprouty2 assembles into large monodisperse spheres containing ≈24 polypeptides per particle. Biochemical experiments indicate that the charge state of the iron within Sprouty2 particles may be insulated from ambient intracellular redox. These features offer the possibility that Sprouty2 particles are capable of receiving, maintaining, and dissipating electrical charge in a manner formally equivalent to a battery.

iron–sulfur | multisubunit | redox

Sprouty proteins were initially discovered as the product of the *Sprouty* gene of *Drosophila melanogaster.* Flies bearing an inactivating mutation in the *Sprouty* gene display enhanced branching morphogenesis in the larval tracheal system (1). Mutations in the *Branchless* and *Breathless* genes attenuate branching morphogenesis. *Branchless* and *Breathless* encode, respectively, the fibroblast growth factor (FGF) and FGF receptor (2, 3). Because Sprouty is an intracellular protein (4), it has been hypothesized that this protein acts as a specific inhibitor of receptor tyrosine kinase signaling (5). Whereas considerable evidence has accumulated in support of this prediction, the precise functional mechanism used by Sprouty to inhibit tyrosine kinase signaling remains unclear. To initiate biochemical experiments pertinent to Sprouty function, we expressed and purified the mammalian Sprouty2 protein. Most fundamental to our observations is the discovery that the conserved cysteine-rich "Sprouty" domain coordinates an iron–sulfur complex. These and other features of the large oligomeric assembly provide evidence that Sprouty proteins contain a dedicated sensing capacity responsive to nitric oxide, redox state, or both.

Methods

Protein Purification. Mouse Sprouty2 was expressed as a maltose-binding protein (MBP) fusion in *Escherichia coli* strain BL21(DE3). The cells were cultured at 37°C until the $A_{600\ nm}$ reached 0.6 and were induced with 0.3 mM isopropyl β-D-thiogalactoside for 3 h before harvest. The cells were suspended in 15 mM Hepes buffer (pH 7.5) containing 200 mM NaCl, 1 mM DTT, and 1 mg/ml lysozyme, incubated on ice for 30 min and sonicated. After spinning in an ultracentrifuge at 30,000 rpm (Beckman rotor Ti75) for 30 min at 4°C, the supernatant was incubated with amylose resin for 2 h and, after washing, bound protein was eluted with 10 mM maltose. To remove the MBP tag, tobacco etch virus protease was incubated with purified fusion protein (1:100 wt/wt) at 4°C overnight, and MBP monomer was separated by gel filtration.

Electron Paramagnetic Resonance (EPR) Spectroscopy. X-band EPR spectra were recorded by using a Bruker (Billerica, MA) model EMX 6/1. Routine EPR measurement conditions were as follows: microwave frequency, 9.34 GHz; microwave power, 3.99 mW; modulation frequency, 100 kHz; modulation amplitude, 20.0 G; sweep field, 1,000 G; sample temperature, 100 K; and receiver gain, 2.83×10^5. The protein concentration was 100 μM.

Determination of Redox Potentials. The redox potential of Sprouty2 was determined at 25°C by using the photoreduction system of Massey and Hemmerich (6). For this, 20–30 μM protein in 0.05 M Hepes buffer, pH 7.4, together with 5 mM EDTA and 1 μM deazariboflavin and redox indicator dye (safranine-O) were mixed together and made anaerobic in a cuvette. A trace amount of oxygen was removed by glucose and glucose oxidase. The reaction was started by shining light on the cuvette, and absorbance spectra were collected after the absorbance was stabilized. The reduction of Sprouty2 was measured at 410 nm (isosbestic point of safranine-O). The percent reduction of safranine-O was calculated from A_{510} after correction for the absorbance of Sprouty2. The redox potential was calculated from the Nernst equation.

Cell Culture. SHEP neuroblastoma cells were cultured in DMEM (Invitrogen) supplemented with 10% FBS and antibiotics. Transfection was carried out using Lipofectamine 2000 (Invitrogen). Cells transfected with GFP constructs were analyzed with a Nikon Eclipse 90i motorized research microscope with Plan Apo lenses and fluorescence and excite illuminator, coupled with METAMORPH IMAGE ACQUISITION (Molecular Devices, Downingtown, PA) software. The Sprouty2 inducible cell line was made by transfection with ecdysone-inducible expression vectors (pIND) encoding ORFs for Sprouty2, along with an expression vector (VgRXR) encoding the human retinoid X receptor (RXR) and a modified *D. melanogaster* ecdysone (VgEcR) receptor. Stable integration of pIND-Sprouty2 and VgRXR expression vectors was achieved by selecting cells for hygromycin and zeocin resistance. Sprouty2-inducible clones were confirmed by Western blotting by using an anti-Sprouty2 antibody.

Analytical Ultracentrifugation. Experiments were performed using a Beckman XL-I analytical ultracentrifuge. Sedimentation velocity data were collected at 280 nm, 20°C, and 42,000 rpm (Beckman rotor Ti75) and analyzed using the second-moment method in the Beckman software. For sedimentation equilibrium experiments, samples were loaded in an An60Ti rotor and run at 6,000 rpm at 4°C. Data were collected at a wavelength of 280 nm. Background absorbance was estimated by overspeeding at 42,000 rpm until a flat baseline was obtained. Analysis of the data, including estimation of molecular weight, was carried out using the Beckman software.

Freely available online through the PNAS open access option.

Abbreviations: FGF, fibroblast growth factor; EPR, electron paramagnetic resonance; SDO, Sprouty domain only; MBP, maltose-binding protein; EM, electron microscopy.

§To whom correspondence should be addressed. E-mail: smckni@biochem.swmed.edu.

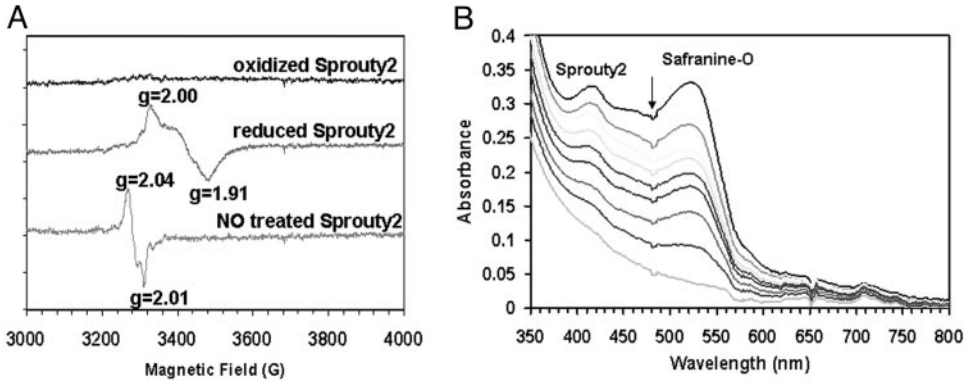

Fig. 1. EPR and redox measurement of Sprouty2 protein. (*A*) EPR spectra of purified Sprouty2 proteins. (Top trace) Oxidized Sprouty2; (middle trace) Sprouty2 anaerobically reduced with 10 mM dithionite; (bottom trace) Sprouty2 after mixing with NO saturated buffer (2 mM). Protein concentrations were ≈100 μM. Experiments were performed by using a Bruker EMX 6/1 spectrometer operating in X-band mode. Conditions: microwave power 3.99 mW, modulation frequency 100 kHz, modulation amplitude 20 G (1 G = 0.1 mT), and temperature 100 K. (*B*) Spectral changes during anaerobic photoreduction of Sprouty2. A solution of Sprouty2 was dissolved in buffer with safranine-O and a catalytic concentration of 5-deazariboflavin and placed in a quartz cuvette under an atmosphere of nitrogen. After each step of photoreduction, a spectral scan was taken subsequent to the point at which the redox state of protein and dye had reached equilibrium. The arrow indicates the absorbance decayed upon photoreduction.

Electron Microscopy (EM). Negative staining revealed uniform globular particles with a diameter of ≈100 Å. Sprouty2–Sprouty domain only (SDO) protein (5 μl at 0.1 mg/ml) was applied to carbon-coated 300-mesh copper grids and stained with 1% uranyl formate. Samples were then viewed with a JEOL 1200 EX electron microscope operating at 80 kV, and images were taken at ×40,000 with a focus range of 2–3 μm under focus. Micrographs were digitized by a Leafscan 45 scanner at a step size of 10 μm, and particles were selected by using the Boxer application of EMAN (7).

Results and Discussion

Visual analysis of purified Sprouty2 gave evidence of an amber color having an absorbance maximum at 415 nm (Fig. 6, which is published as supporting information on the PNAS web site). Coloration of the protein was determined to reflect the presence of an iron–sulfur complex as deduced by inductively coupled plasma[¶] and chemical analysis of free sulfur (8). The molar ratios of both iron and sulfur were consistent with a [2Fe−2S] complex. As shown in Fig. 1*A*, EPR spectroscopy of reduced Spouty2 revealed reduction-dependent peaks with *g* values of 2.00 and 1.91. This spectral pattern matches those of many other proteins having dedicated [2Fe−2S] complexes (9, 10). In retrospect, it is not surprising that Sprouty2 is a metal-binding protein. The conserved "Sprouty domain" of all family members contains 17 invariant cysteine residues (Fig. 7, which is published as supporting information on the PNAS web site) (11).

Proteins containing an iron–sulfur complex are often subject to nitrosylation by nitric oxide (NO) (12). Exposure of purified Sprouty2 to NO yielded a distinct change in EPR spectrum, yielding new peaks at *g* values of 2.04 and 2.01. This altered EPR spectrum is consistent with nitrosylation of Sprouty2 at iron residues, thereby eliminating free sulfur. Nitrosylation of Sprouty2 was irreversible and saturable at gas levels nearly equimolar to protein levels.

The data presented in Fig. 1*A* give evidence that Sprouty2 can exist in an oxidized, reduced, or nitrosylated state. To measure the redox potential at which iron within the iron–sulfur complex converts from the oxidized to reduced state, Sprouty2 was mixed with safranine-O and subjected to photoreduction (Fig. 1*B*) (6). Spectrophotometric scans taken as a function of time over the course of photoreduction gave evidence of a relatively well matched diminution in adsorbance, indicating that Sprouty2 became reduced at a slightly more negative redox potential (−310 mV) than the safranine-O standard (−289 mV). These data give evidence that the iron–sulfur complex associated with Sprouty2 is poised at a similar redox potential to well characterized sensory proteins that use an iron–sulfur complex as a dedicated redox sensor (13).

Transgenic fruit fly larvae expressing inducible NO synthase have been reported to exhibit a phenotype of enhanced tracheal branching not unlike that seen in *sprouty* mutants (14). Moreover, L-NAME, a selective antagonist of the production of endogenous NO, has been reported to impede branching morphogenesis in fruit fly larvae (14). Knowing that NO binds irreversibly to the iron–sulfur complex of Sprouty2 (Fig. 1*A*), we tested the effects of NO on FGF signaling in cultured cells. Neuroblastoma cells were programmed to conditionally induce Sprouty2 in response to ponasterone (15). Consistent with numerous previous studies (16, 17), expression of Sprouty2 led to an attenuation of FGF signaling, as deduced by intracellular levels of phosphorylated ERK (Fig. 2). Exposure of cultured neuroblastoma cells to a short-lived NO donor derepressed Sprouty2-mediated inhibition of pERK. Such observations indicate that nitrosylation of Sprouty2 may overcome its inhibition of FGF signaling, consistent with the aforementioned studies of NO effects on branching morphogenesis in fruit fly larvae.

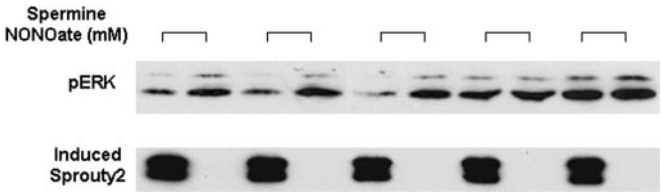

Fig. 2. NO effect on Sprouty2-mediated inhibition of FGF signaling. V5-tagged Sprouty2 was induced with ponasterone (250 ng/ml) for 16 h, and cells were treated with spermin-nonoate for 2 h before exposure to FGF. Ten minutes after adding FGF (50 ng/ml), whole-cell lysate was collected for Western blot analysis. ERK activation was monitored with anti-phospho-ERK antibody, and Sprouty2 expression was confirmed by Western blotting using an anti-V5 antibody.

[¶]Iron content was measured by inductively coupled plasma at the Southern Spectrographic Laboratory (Irving, TX). Protein concentration was determined by absorption at 280 nm. The ratio between iron and protein was ≈2:1.

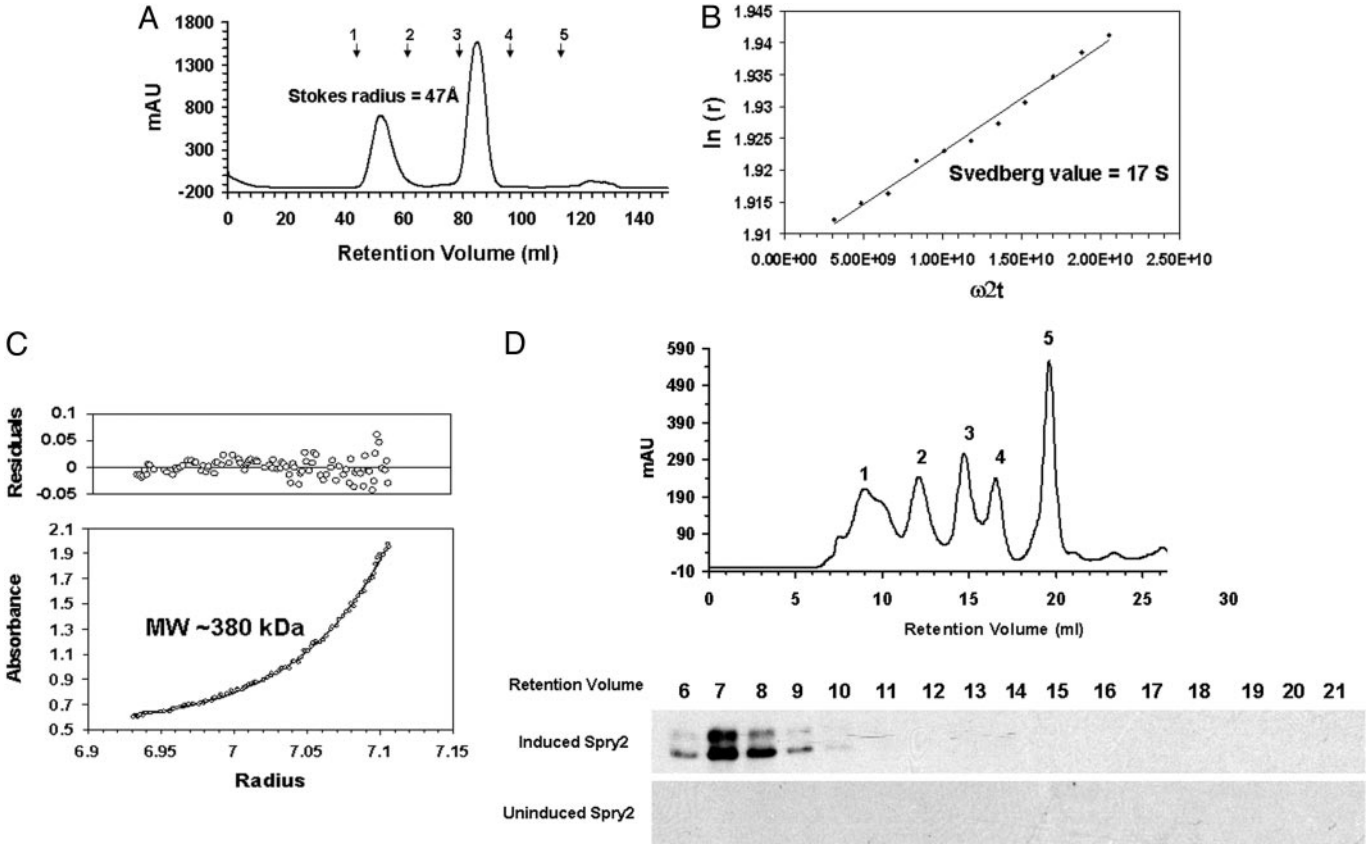

Fig. 3. Physical properties of Sprouty2-SDO protein. Gel filtration, velocity sedimentation, and equilibrium sedimentation revealed a monodisperse protein complex consisting of 20–24 subunits. (*A*) Sprouty2-SDO migrates as a single peak within a Superdex 200 column with an elution volume corresponding to a Stokes radius of 47 Å. Arrows on the FPLC trace indicated retention volume of protein standards. 1, thyroglobulin, 670 kDa; 2, gammaglobulin, 158 kDa; 3, ovalbumin, 44 kDa; 4, myoglobin, 17 kDa; and 5, vitamin B12, 1.35 kDa. (*B*) Velocity sedimentation second-moment plot revealed a sedimentation coefficient of 17S for the Sprouty2-SDO particle. This value, combined with a Stokes radius of 47 Å, yielded a calculated molecular mass of 340 kDa for the Sprouty2-SDO particle. (*C*) Equilibrium sedimentation independently predicted a molecular mass of 380 kDa. Data were analyzed using the single ideal species model of the ORIGIN 6.0 software (Beckman). (*D*) Gel filtration elution profile of full length Sprouty2 synthesized from inducible neuroblastoma cells. Induced and uninduced Sprouty2 cell lysate was prepared in 50 mM Tris buffer, pH 7.4/150 mM NaCl/1 mM DTT/1% Nonidet P-40. After injection into a Superdex 200 column, fractions (1 ml each) between 6 and 21 ml of column retention volume were collected and assayed by Western blotting using anti-Sprouty2 antibody. No signal was detected from uninduced cell lysate. Molecular weight standards used in FPLC trace (*Upper*) are same as in *A*.

Purified SDO of Sprouty2‖ was further characterized by gel filtration as a means of establishing its mono- or oligomeric state. After proteolytic liberation of Sprouty2-SDO from MBP, Sprouty2-SDO was observed to elute from a standard gel filtration column with an apparent molecular mass much larger than anticipated (Fig. 3*A*). Unlike MBP, which eluted as an apparent monomer according to calibration by molecular weight standards, recombinant Sprouty2-SDO eluted at a position corresponding to a Stokes radius of 47 Å. Sprouty2 in cell extracts prepared from neuroblastoma cells eluted from the gel filtration at a corresponding fraction (Fig. 3*D*). Apparently, Sprouty2 derived from both bacterial and mammalian sources assembles as an unusually large protein complex.

The oligomeric state of Sprouty2-SDO was further characterized by velocity and equilibrium sedimentation in an analytical ultracentrifuge (Fig. 3 *B* and *C*). Velocity sedimentation gave evidence of a monodisperse particle having a Svedberg value of 17 S. Coupled with a Stokes radius of 47 Å as deduced by gel filtration, these data predict a molecular mass of 340 kDa (18). As shown in Fig. 3*C*, such observations were confirmed by equilibrium sedimentation, independently allowing calculation of a particle mass of 380 kDa. Importantly, both velocity and equilibrium sedimentation studies gave evidence of particles of a monodisperse size.

That Sprouty2 forms large homogenous particles was confirmed by EM. Purified protein was applied to thin carbon film on EM grids and negatively stained by using uranyl formate. Fig. 4*A* shows the EM image of a field containing hundreds of unselected Sprouty2 oligomers. Particle dimensions were measured on ≈5,000 particles, yielding an average particle radius of ≈45–50 Å (Fig. 4*B*). Higher-magnification images of 60 individual particles are shown in Fig. 4*C*. These EM studies reveal a roughly spherical, monodisperse particle exhibiting a size corresponding to the molecular mass predicted by the combination of gel filtration and analytical ultracentrifugation.**

‖Proteolytic liberation of full-length Sprouty2 from MBP resulted in partial precipitation of Sprouty2. As such, subsequent studies, including gel filtration, analytical ultracentrifugation, and EM, were conducted by using a fragment limited to the conserved cysteine-rich Sprouty domain. This fragment was composed of residues 179–315 of the mouse Sprouty2 polypeptide (Fig. 7). TEV protease cleavage of the MBP-SDO fusion protein liberated a fully soluble SDO polypeptide (Fig. 8, which is published as supporting information on the PNAS web site). This SDO fragment of Sprouty2 behaved indistinguishably from full length MBP-Sprouty2 protein.

**Negative staining EM revealed spherical particles with radii of 45–50 Å. The volume of a spherical protein complex is equal to its mass multiplied by its partial specific volume. Therefore, the observed radius of 47 Å predicts a molecular mass of 360 kDa, a value that agrees with particle size calculations obtained independently by gel filtration, velocity sedimentation, and equilibrium sedimentation.

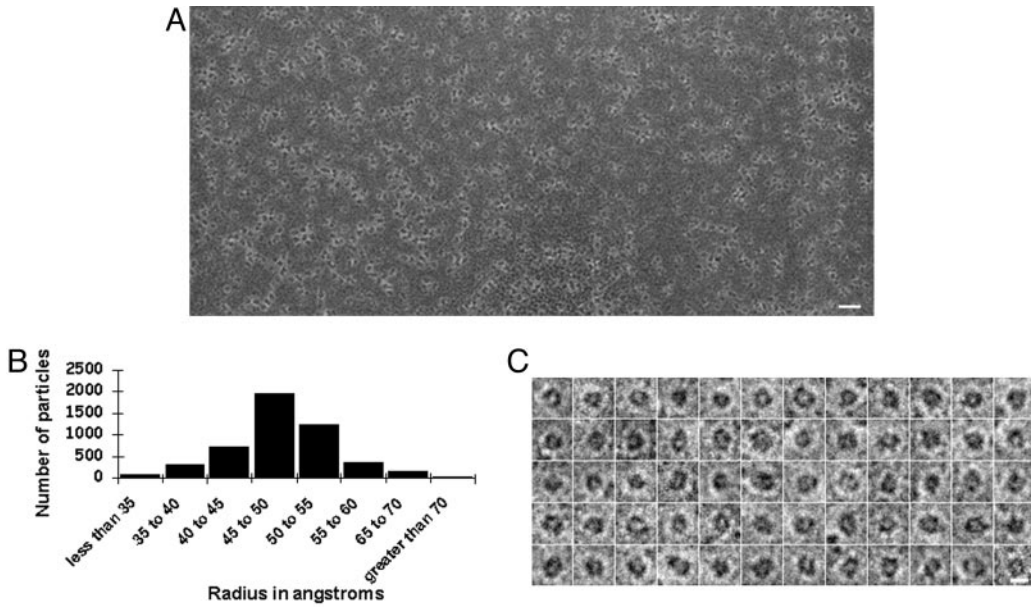

Fig. 4. EM images of Sprouty2-SDO proteins particles. (*A*) Sprouty2-SDO proteins appear as discreet spherical particles when observed by EM. (Bar, 500 Å.) (*B*) Histogram showing variation in radius of Sprouty2 particles. Over 80% of particles examined exhibited a radius between 40 and 55 Å. The average radius as measured by EM closely matched the Stokes radius obtained by gel filtration (47 Å). (*C*) Magnified images of representative Sprouty-SDO particles. (Bar, 100 Å.)

Numerous previous immunohistochemical studies of various Sprouty proteins have given evidence of punctate cytoplasmic staining (19). Neuroblastoma cells expressing a Sprouty2:GFP fusion protein were examined by light microscopy, revealing a distinctly punctate pattern of fluorescence (Fig. 5 *Upper*). By contrast, a GFP-tagged derivative of Sprouty2 lacking its conserved cysteine-rich Sprouty domain yielded diffuse staining throughout the cytoplasm (Fig. 5 *Lower*). Thus, irrespective of whether studied by gel filtration, ultracentrifugation, EM, or light microscopy, mammalian Sprouty2 appears to assemble into large, particulate protein aggregates.

Observations reported herein provide evidence that the mammalian Sprouty2 protein contains an iron–sulfur complex having a redox potential of −310 mV. This redox potential closely matches that of the SoxR transcription factor of *E. coli*, which utilizes its iron–sulfur complex to sense the redox state and facilitate appropriate transcriptional adaptation to an aberrantly oxidized intracellular redox environment (13). Although optimally poised at −310 mV to serve as a redox sensor, the iron–sulfur complex present in the Sprouty2 protein particle appears, paradoxically, to be insulated from intracellular redox. When iron within the Sprouty2 complex is oxidized, we have been unable to reduce it even upon exposure to the strongest of intracellular reductants, including NADPH (−320 mV). Likewise, when reduced either by dithionite or photoreduction, the iron–sulfur complex within the Sprouty2 particle is immune to oxidation, even upon exposure to molecular oxygen.[††]

In what way might these observations relate to the means by which Sprouty proteins inhibit receptor tyrosine kinase signaling? We hypothesize that NO binding to the iron–sulfur complex may be responsible for impeding the inhibitory role of Sprouty2 of FGF signaling, as shown in Fig. 2. These observations, at present, offer no more than an indirect connection between NO and the regulatory action of Sprouty2. That NO binds to the iron–sulfur complex of Sprouty2 in test tube reactions is strongly supported by the EPR data provided herein. Likewise, interpretation of the direct derepressive role of NO on Sprouty2 is consistent with the observations of Wingrove and O'Farrell (14), who have found that NO phenocopies the *sprouty* mutation in fruit flies. If these interpretations prove correct, we offer the speculation that electronic modulation via the iron–sulfur complex present in Sprouty2 may be at the heart of its action as an intracellular modulator of receptor tyrosine kinase signaling.

Finally, for what reason might Sprouty2 assemble into unusually large monodisperse particles? We hypothesize that the spherical assemblies may somehow insulate the electronics of the complex from ambient intracellular redox fluctuation. If so, individual particles might be hysteretic; battery-like, by insulating a specific charge state until coupled to the proper receptacle.

In searching the biochemistry literature for precedent studies instructive to the paradoxical observations reported herein, we were reminded of the complex organization of pyruvate dehydro-

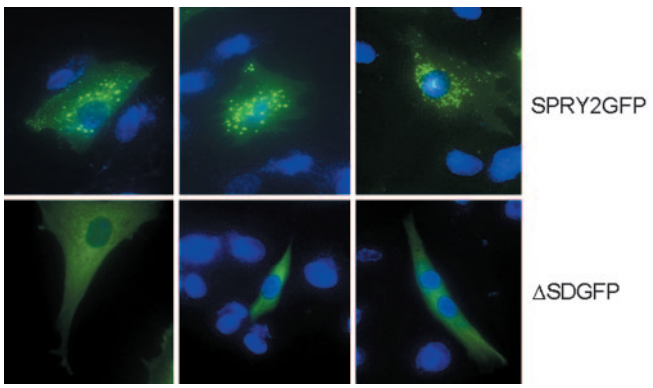

Fig. 5. Punctate distribution of Sprouty2 in neuroblastoma cells. SHEP cells were transiently transfected with plasmids encoding GFP-Sprouty2 (*Upper*) or GFP-truncated Sprouty2 lacking the conserved cysteine-rich Sprouty domain (*Lower*). The latter variant of Sprouty2 was manipulated to remove residues 179–315 (Fig. 7). Transfection, cell culture, and fluorescence imaging methods are described in *Methods*.

[††]After reduction of the Sprouty2 protein anaerobically, the sample was exposed to ambient atmosphere. Based on spectroscopic measurement of oxidized iron, no evidence of reoxidation was observed after >4 hours of O_2 exposure.

genase. This multifunctional enzyme utilizes a sophisticated electron transport chain to oxidatively convert pyruvate into acetyl-CoA and NADH (20–22). At the core of the pyruvate dehydrogenase complex is a homomeric aggregate consisting of 24 E2 subunits specifying the dihydrolipolyl transacetylase function of the enzyme. Each E2 subunit is appended with three lipoic acid chains, endowing the 24-subunit core of the enzyme with 144 cysteine residues critical for efficient electron and acetyl group transport. The Sprouty2 particles described herein also appear to be composed of ≈24 subunits, each containing an iron–sulfur complex. Additionally, each Sprouty2 subunit contains 13 invariant cysteine residues not involved in metal chelation, meaning that the intact particle contains upwards of 312 free cysteine residues potentially available for electron transport.[‡‡]

[‡‡]Human, mouse, and fly sprouty proteins share 17 perfectly conserved cysteine residues. Typical [2Fe−2S] clusters require four cysteine residues for metal chelation, leaving 13 of 17 conserved cysteines free. All mammalian sprouty proteins contain 20 conserved cysteines, meaning that the calculation of 13 free cysteine residues within each subunit of the particle might represent an underestimation.

We close with two predictions: First, that the present study offers an initial description of the central core of a complex enzyme not unlike pyruvate dehydrogenase. Second, we speculate that identification of the biologically relevant polypeptide receptacles to this Sprouty particle will lead to the discovery of a signaling switch having a sufficiently challenging energetic threshold to require electron transport.

We thank Pat O'Farrell, Squire Booker, and Tom Roche for critical review of this manuscript; Leeju Wu for technical assistance; Derk Binns, Nicholas Malmquist, and Joseph Albanesi for help with analytical ultracentrifugation; Julian Peterson for extensive help with redox measurement; and Charles Dann, Benjamin Tu, Zbyszek Otwinowski, and Christopher Colbert for valuable scientific input. This work was supported by funds provided to S.L.M. by the National Institute of Mental Health (R01-4R37MH59388), a Director's Pioneer Award from the National Institutes of Health (5DP10D000276), the Morton H. Meyerson Family Tzedakah Fund, and unrestricted funds from an anonymous donor.

1. Hacohen, N., Kramer, S., Sutherland, D., Hiromi, Y. & Krasnow, M. A. (1998) *Cell* **92,** 253–263.
2. Klambt, C., Glazer, L. & Shilo, B. Z. (1992) *Genes Dev.* **6,** 1668–1678.
3. Sutherland, D., Samakovlis, C. & Krasnow, M. A. (1996) *Cell* **87,** 1091–1101.
4. Casci, T., Vinos, J. & Freeman, M. (1999) *Cell* **96,** 655–665.
5. Kim, H. J. & Bar-Sagi, D. (2004) *Nat. Rev. Mol. Cell. Biol.* **5,** 441–450.
6. Massey, V. & Hemmerich, P. (1978) *Biochemistry* **17,** 9–16.
7. Ludtke, S. J., Baldwin, P. R. & Chiu, W. (1999) *J. Struct. Biol.* **128,** 82–97.
8. Beinert, H. (1983) *Anal. Biochem.* **131,** 373–378.
9. Raux-Deery, E., Leech, H. K., Nakrieko, K. A., McLean, K. J., Munro, A. W., Heathcote, P., Rigby, S. E., Smith, A. G. & Warren, M. J. (2005) *J. Biol. Chem.* **280,** 4713–4721.
10. Pan, G., Menon, A. L. & Adams, M. W. (2003) *J. Biol. Inorg. Chem.* **8,** 469–474.
11. Lim, J., Yusoff, P., Wong, E. S., Chandramouli, S., Lao, D. H., Fong, C. W. & Guy, G. R. (2002) *Mol. Cell. Biol.* **22,** 7953–7966.
12. Drapier, J. C. (1997) *Methods* **11,** 319–329.
13. Hidalgo, E., Ding, H. & Demple, B. (1997) *Trends Biochem. Sci.* **22,** 207–210.
14. Wingrove, J. A. & O'Farrell, P. H. (1999) *Cell* **98,** 105–114.
15. Reick, M., Garcia, J. A., Dudley, C. & McKnight, S. L. (2001) *Science* **293,** 506–509.
16. Hanafusa, H., Torii, S., Yasunaga, T. & Nishida, E. (2002) *Nat. Cell. Biol.* **4,** 850–858.
17. Impagnatiello, M. A., Weitzer, S., Gannon, G., Compagni, A., Cotten, M. & Christofori, G. (2001) *J. Cell Biol.* **152,** 1087–1098.
18. Siegel, L. M. & Monty, K. J. (1966) *Biochim. Biophys. Acta* **112,** 346–362.
19. Tsumura, Y., Toshima, J., Leeksma, O. C., Ohashi, K. & Mizuno, K. (2005) *Biochem. J.* **387,** 627–637.
20. Mattevi, A., Obmolova, G., Schulze, E., Kalk, K. H., Westphal, A. H., de Kok, A. & Hol, W. G. (1992) *Science* **255,** 1544–1550.
21. Patel, M. S. & Roche, T. E. (1990) *FASEB J.* **4,** 3224–3233.
22. Milne, J. L., Shi, D., Rosenthal, P. B., Sunshine, J. S., Domingo, G. J., Wu, X., Brooks, B. R., Perham, R. N., Henderson, R. & Subramaniam, S. (2002) *EMBO J.* **21,** 5587–5598.